MICROWAVE ABSORPTION OF ELECTROMAGNETIC RADIATION IN THIN MAGNETIC FILMS AND FeNi –BASED MULTILAYERED STRUCTURES DESIGNED FOR APPLICATIONS

Sergei V. Shcherbinin[1,2], Stanislav O. Volchkov[1], Andrey V. Svalov[1], Galina V. Kurlyandskaya[1,3]

[1]Ural Federal University, Mira 19, Ekaterinburg, 620002, Russia

[2]Institute of Electrophysics, Amundsen str., 106, Ekaterinburg, 620016, Russia

[3]Universidad del País Vasco UPV-EHU, Depto Electricidad y Electrónica, Leioa, 48940, Spain

Abstract

Thin magnetic films and multilayered structures are of specific interest for the development of small magnetic field detectors and biosensors. Some of these devices are operating in the microwave range in other cases characterization by microwave techniques is necessary to gain the material understanding. We consider the resonance absorption of electromagnetic waves in the microwave range, depending on the composition of the magnetron sputtered FeNi-based magnetic films suitable for magnetoimpedance sensor applications. Particular attention is paid to the matching of the high-frequency path for multilayers.

Key words: *magnetic multilayers, giant magnetoimpedance, microwave absorption, ferromagnetic resonance, magnetic field sensors*

1. INTRODUCTION

Magnetoimpedance phenomenon consists in the change of the total impedance of ferromagnetic conductor under application of external magnetic field [1, 2, 3]. This effect attracted attention of the scientific community due to possible sensor applications [4, 5, 6]. Significant progress was achieved in the study of giant magneto-impedance (GMI) of thin ferromagnetic films [7, 8]. Thin film geometry – is the most suitable technological solution due to excellent compatibility with present day semiconductor technology [6, 7].

There are different techniques for high frequency characterization of soft magnetic materials. As the first step structural and quasistatic characterization is always requested. For magnetization dynamics ferromagnetic resonance (FMR) techniques are very useful. FMR describes resonant absorption of electromagnetic radiation in a magnetic material. Absorption is measured as a function of an external applied field [9]. FMR is characterized by the resonance field (H_{res}) and the line width (ΔH). Measurements of the resonance field at several frequencies can be useful for evaluation of such parameters as magnetization and magnetic anisotropy. One of the well-known techniques for FMR studies is the cavity perturbation method [10].

Characterization of the samples of the same multilayered film structures in the microwave range using broad band techniques [11, 12] become more complex as the parameters of the holder begin to contribute to the absorption rate and they therefore must be taken into account. Since the holders are made of fiberglass, the actual measurement range is limited to a frequency of *3 GHz*. However, the results of calculations and modelling determine the possibility of correct measurements at frequencies up to *10 GHz*. Therefore, it is possible to extend the frequency range by using a more suitable (although more expensive materials) as a microstrip line substrates.

In this work, the entire microwave path consisting of the sample holder and the sample itself was considered and studied. We had developed special method for the extracting of the parameters of a transmission line formed by a sample on the substrate. The phenomenon of resonant absorption of electromagnetic waves in the multi-layered film based sample in the external applied magnetic field was carefully investigated. The experimental absorption curves were in a good agreement with the known FMR responses in a given metal in a frequency range up to *3 GHz*.

2. EXPERIMENTAL PROCEDURE AND RESULTS

2.1. Sample preparation and characterization techniques

The FeNi(70 nm)Cu(3 nm) FeNi(70 nm)/Cu(500 nm)/FeNi(70 nm)Cu(3 nm)FeNi(70 nm) multilayers were deposited onto Corning glass substrates by the method of high frequency ion-plasma deposition in an argon atmosphere from the alloyed $Fe_{19}Ni_{81}$ or Cu targets. Preliminary vacuum before the deposition was 2×10^{-6} *Torr* and the working pressure of argon was 1×10^{-3} *Torr*. The thickness of each layer was determined by the deposition time (with allowance for the data of preliminary calibration using an atomic force microscope). The deposition rates were *0.13 nm/s* for permalloy and *0.23 nm/s* for copper. Metallic masks were used to insure the rectangular shape of the multilayered elements. FeNi-based element dimensions were *0.5 mm* × *11 mm*, Cu-contacts dimensions were *1.5 mm* × *1.8 mm*. More technical details can be found elsewhere [13]. Thick copper contacts (about *500 nm*) were sputtered after the FeNi-based multilayers deposition. To obtain well defined transverse magnetic anisotropy with low dispersion of the local effective anisotropy constant, the depositions were performed in a constant magnetic field H_{dep} = *100 Oe* applied parallel to the short side and in-plane of the multilayered elements.

Magnetic characterization of the multilayers consisted in the measurements of the hysteresis loops for the external magnetic field applied in-plane of the rectangular element in the direction parallel to the long side of the element. All elements had well defined transverse magnetic anisotropy with the anisotropy field of the order of *5-7 Oe* and very low coercivity of the order of *1 Oe*. After deposition and magnetic characterization, the multilayered elements were installed into the sample holder (microstrip line) using highly conductive silver glue (Fig. 1).

The microwave studies of the multilayered structures were done with a specially designed installation on the basis of the Rohde & Schwarz ZVA-67 Vector Network Analyzer (VNA) with possibility of application of the external magnetic field up to *15 kOe* [14].

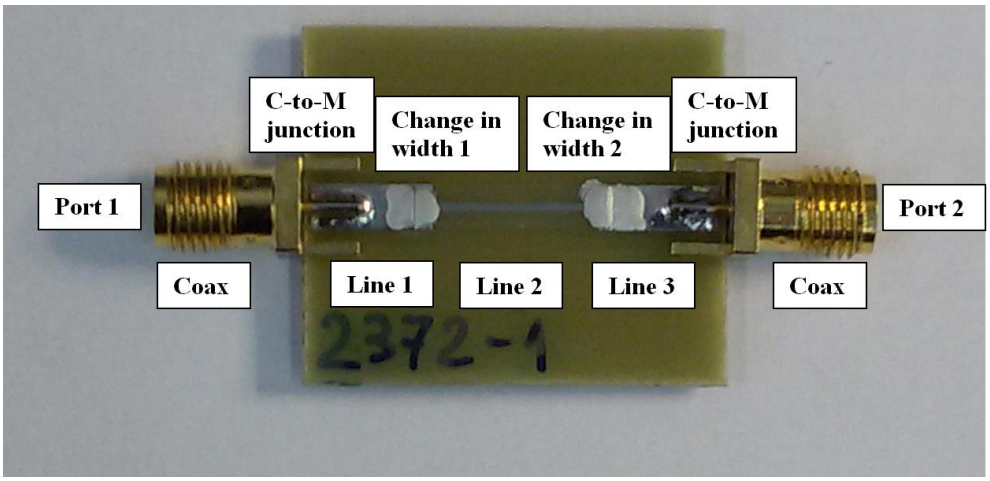


Fig. 1. General view of the multilayered FeNi(70 nm)Cu(3 nm) FeNi(70 nm)/Cu(500 nm)/FeNi(70 nm)Cu(3 nm)FeNi(70 nm) rectangular element installed into the sample holder. Characteristic subdivisions of the equivalent circuit used for calculations are also indicated

A ferromagnetic *0.5 mm* wide structure deposited onto a glass substrate with a thickness of *0.2 mm*, forms a microwave transmission line. Since it is mounted onto textolite with one side foil plate, one can be approximate the structure as Line 2 microstrip line. In order to determine the parameters of a given line, it is necessary to compile an equivalent circuit of the entire holder. The holder is linked by Subminiature version A (SMA) connectors to the VNA coaxial cable connectors, which are being carefully calibrated. Therefore, we can assume that the VNA measurement is from port 1 to port 2 (Fig. 1).

2.2. Modelling parameters definitions

For the preliminary calculation, we can assume that the dimensions of the inhomogeneities are much smaller than the wavelength and represent an equivalent circuit in the form of a series connection of four-terminal networks characterized by *ABCD*-parameters (Fig. 2). M_X matrices of *ABCD*-parameters were defined as follows:

$M_R = \begin{bmatrix} A & B \\ C & D \end{bmatrix}_R$ *ABCD* matrix of the **Coaxial connector**.

$M_{P1} = \begin{bmatrix} A & B \\ C & D \end{bmatrix}_{P1}$ *ABCD* matrix of the **Coaxial-to-Microstrip junction 1**.

$M_{L1} = \begin{bmatrix} A & B \\ C & D \end{bmatrix}_{L1}$ *ABCD* matrix of the microstrip **Line 1**.

$M_{T1} = \begin{bmatrix} A & B \\ C & D \end{bmatrix}_{T1}$ *ABCD* matrix of the **Change in width 1** of the microstrip line.

$M_2 = \begin{bmatrix} A & B \\ C & D \end{bmatrix}_2$ *ABCD* matrix of the ferromagnetic structure **Line 2**.

$M_{T2} = \begin{bmatrix} A & B \\ C & D \end{bmatrix}_{T2}$ *ABCD* matrix of the **Change in width 2** of the microstrip line.

$M_{L3} = \begin{bmatrix} A & B \\ C & D \end{bmatrix}_{L3}$ *ABCD* matrix of the microstrip **Line 3**.

$M_{P2} = \begin{bmatrix} A & B \\ C & D \end{bmatrix}_{P2}$ *ABCD* matrix of the **Coaxial-to-Microstrip junction 2**.

$M_R = \begin{bmatrix} A & B \\ C & D \end{bmatrix}_R$ *ABCD* matrix of the **Coaxial connector**.

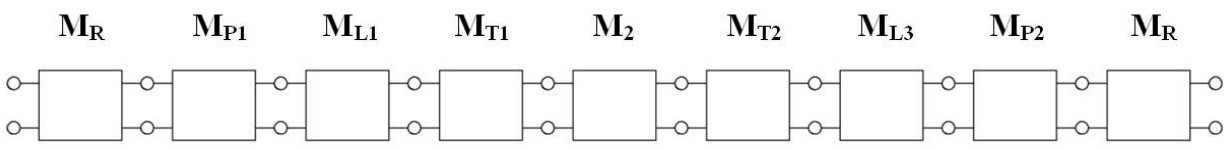


Fig. 2. Equivalent circuit, where M_X – matrices of *ABCD*-parameters

Using VNA, we measure the *S*-parameters of the entire system (the holder with the sample). From the *S*-parameters of the whole system it is necessary to find the parameters of the ferromagnetic sample represented as the matrix: $\begin{bmatrix} A & B \\ C & D \end{bmatrix}_2$

ABCD matrix of the whole system can be obtained from the *S*-parameters as follows [15]:

$$A = \frac{(1 + S_{11}) \cdot (1 - S_{22}) + S_{12} \cdot S_{21}}{2 \cdot S_{21}}$$

$$B = Z_0 \cdot \frac{(1 + S_{11}) \cdot (1 + S_{22}) - S_{12} \cdot S_{21}}{2 \cdot S_{21}}$$

$$C = \frac{1}{Z_0} \cdot \frac{(1 - S_{11}) \cdot (1 - S_{22}) - S_{12} \cdot S_{21}}{2 \cdot S_{21}}$$

$$D = \frac{(1 - S_{11}) \cdot (1 + S_{22}) + S_{12} \cdot S_{21}}{2 \cdot S_{21}}$$

Supposing that all the parameters of the holder are known we can write following relations:

$$\begin{bmatrix} A & B \\ C & D \end{bmatrix}_1 = \begin{bmatrix} A & B \\ C & D \end{bmatrix}_R \cdot \begin{bmatrix} A & B \\ C & D \end{bmatrix}_{P1} \cdot \begin{bmatrix} A & B \\ C & D \end{bmatrix}_{L1} \cdot \begin{bmatrix} A & B \\ C & D \end{bmatrix}_{T1}$$

$$\begin{bmatrix} A & B \\ C & D \end{bmatrix}_3 = \begin{bmatrix} A & B \\ C & D \end{bmatrix}_{T2} \cdot \begin{bmatrix} A & B \\ C & D \end{bmatrix}_{L3} \cdot \begin{bmatrix} A & B \\ C & D \end{bmatrix}_{P2} \cdot \begin{bmatrix} A & B \\ C & D \end{bmatrix}_R$$

$$\begin{bmatrix} A & B \\ C & D \end{bmatrix}_S = \begin{bmatrix} A & B \\ C & D \end{bmatrix}_1 \cdot \begin{bmatrix} A & B \\ C & D \end{bmatrix}_2 \cdot \begin{bmatrix} A & B \\ C & D \end{bmatrix}_3$$

Therefore, finally write down the magnetic sample parameters as follows:

$$\begin{bmatrix} A & B \\ C & D \end{bmatrix}_2 = \begin{bmatrix} A & B \\ C & D \end{bmatrix}_1^{-1} \cdot \begin{bmatrix} A & B \\ C & D \end{bmatrix}_S \cdot \begin{bmatrix} A & B \\ C & D \end{bmatrix}_3^{-1}$$

2.3. Determining the parameters of the holder in the frequency range from 0.1 to 6 GHz

2.3.1. ABCD matrix of the coaxial connector SMA S-P2152

It is known [16] that *ABCD* matrix for the coaxial SMA S-P2152 connector can be written as follows:

$$\begin{bmatrix} A & B \\ C & D \end{bmatrix}_R = \begin{bmatrix} Ch & Z_0 \cdot Sh \\ \frac{Sh}{Z_0} & Ch \end{bmatrix}$$

where $Ch = \cosh(\gamma \cdot length),\ Sh = \sinh(\gamma \cdot length), \gamma = \alpha + i \cdot \beta;$

$\alpha = 0$ – losses are absent; $\beta = \frac{2 \cdot \pi}{\lambda}$; λ – wavelength of the electromagnetic field

2.3.2. ABCD matrix of the coax-to-microstrip junction

Fig. 3 shows the scheme for the electronic circuit corresponding to the coaxial-to-microstrip junction. ABCD matrix of the coaxial-to-microstrip junction can be written as follows:

$$\begin{bmatrix} A & B \\ C & D \end{bmatrix}_P = \begin{bmatrix} 1 + \frac{Y2}{Y3} & \frac{1}{Y3} \\ Y1 + Y2 + \frac{Y1 \cdot Y2}{Y3} & 1 + \frac{Y1}{Y3} \end{bmatrix}$$

where $Y1 = i \cdot \omega \cdot C_p$ $Y2 = i \cdot \omega \cdot C_p$ $Y3 = \frac{1}{i \cdot \omega \cdot L_p}$

Cp = 0.022 pF is the equivalent circuit capacitance and *Lp* = 0.057 nH is the equivalent circuit inductance [17], ω is the circular frequency.

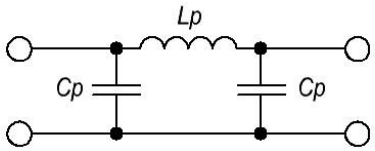


Fig. 3. Equivalent circuit scheme corresponding to the coaxial-to-microstrip junction

2.3.3. ABCD matrix of the microstrip line

ABCD matrix for the microstrip line can be written as follows [16]

$$\begin{bmatrix} A & B \\ C & D \end{bmatrix}_L = \begin{bmatrix} Ch & Zc \cdot Sh \\ \frac{Sh}{Zc} & Ch \end{bmatrix}$$

where $Ch = \cosh(\gamma \cdot length)$, $Sh = \sinh(\gamma \cdot length)$; γ – is the line propagation constant.

$\varepsilon = 4.7$ – relative dielectric constant of textolite; *length = 8 mm* – length of the micrtostrip line; *W = 3 mm* – width of the Cu stripe.

The characteristic impedance of the line is the ratio of the transverse components of the electric and magnetic fields (the transverse components being those at right angles to the direction of propagation). The characteristic impedance of the microstrip line (Z_C) can be calculated as follows:

$$Z_C = \frac{376.7}{\sqrt{\varepsilon_r}} \cdot \left(\frac{We}{h} + 1.393 + 0.667 \cdot \ln\left(\frac{We}{h} + 1.444\right)\right)^{-1} \qquad Z_C = 46.3 \text{ Ohm}$$

$$Q = \frac{\varepsilon - 1}{2} \cdot \frac{t}{h} \cdot \left(\frac{W}{h}\right)^{-0.5} \qquad Q = 8.81 \cdot 10^{-3} \qquad F = \left(1 + \frac{10 \cdot h}{W}\right)^{-0.5} \qquad F = 0.412$$

Effective relative permittivity (ε_r) can be calculated as follows:

$$\varepsilon_r = \frac{\varepsilon + 1}{2} + \frac{\varepsilon - 1}{2} \cdot F - Q \qquad \varepsilon_r = 3.6$$

Let us discuss some parameters of the line propagation constant $\gamma = \alpha + i \cdot \beta$:

The total losses (α), are composed of losses in the conductor (α_w) and losses in the dielectric (α_d): $\alpha = \alpha_w + \alpha_d$. Losses in the conductor can be calculated in accordance with equation:

$$\alpha_W = \frac{6.1 \cdot 10^{-5}}{8.686} \cdot A \cdot \frac{R_S \cdot Z \cdot \varepsilon_r}{h} \cdot \left(\frac{We}{h} + \frac{0.667 \cdot We}{h} \cdot \left(\frac{We}{h} + 1.444\right)^{-1}\right)$$

where $B = h$; $B = 1.47 \cdot 10^{-3}$

$$A = 1 + \frac{h}{We} \cdot \left(1 + \frac{1}{\pi} \cdot ln\left(\frac{2 \cdot B}{t}\right)\right) \qquad \rho = 1.77 \cdot 10^{-8} \ \ Ohm{\cdot}m, \text{ resistivity of copper;}$$

$R_S = \sqrt{\pi \cdot f \cdot \mu_0 \cdot \rho}$ *Ohm*, is the surface resistance of copper.

For example, for the frequency *f = 1 GHz*, $\alpha_W = 0.039$ *Np/m*.

Losses in the dielectric depend on the frequency and they can be calculated in accordance with equation:

$$\alpha_d = \frac{27.3}{8.686} \cdot \frac{\varepsilon}{\varepsilon - 1} \cdot \frac{\varepsilon_r - 1}{\sqrt{\varepsilon_r}} \cdot \frac{tg\delta}{\lambda_0} \ \ Np/m$$

$tg\delta = 10^{-4}$ for *f = 1 GHz*, and therefore $\alpha_d = 0.0034\ Np/m$ and $\alpha = 0.042\ Np/m$.

Line phase coefficient is defined as $\beta = \frac{2 \cdot \pi}{\lambda_0}$

for the wavelength in the line $\lambda_0 = \frac{c}{\sqrt{\varepsilon_r} \cdot f}$

For example, for the frequency *f = 1 GHz*, $\gamma = 0.042 + i \cdot 39.754$

$$A_{L1} = \begin{bmatrix} 0.95 + i \cdot 1.052 & 0.015 + i \cdot 14.47 \\ 6.9 \cdot 10^{-6} + i \cdot 6.76 \cdot 10^{-3} & 0.95 + i \cdot 1.052 \end{bmatrix}$$

2.3.4. ABCD matrix of the change in width 1 of the microstrip line

Let us now estimate the change in width 1 of the microstrip line. Fig. 4 shows the equivalent circuit scheme with discontinuities in width. If the stripe width is 3 mm, Z_{C1} = *46.2 Ohms*. The change of the stripe width for about 0.5 mm causes the change in the characteristic impedance to Z_{C2} = *104.9 Ohms.*

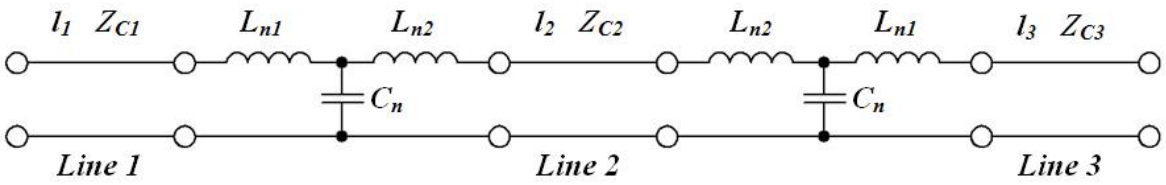


Fig. 4. Equivalent circuit of a sample with discontinuities in the form of changes in width

Let us again write the expression for the *ABCD* matrix:

$$\begin{bmatrix} A & B \\ C & D \end{bmatrix}_T = \begin{bmatrix} 1+\frac{Z1}{Z3} & \frac{Z1\cdot Z2}{Z3}+Z1+Z2 \\ \frac{1}{Z3} & 1+\frac{Z2}{Z3} \end{bmatrix}$$

where $Z1 = i\cdot\omega\cdot L_{n1}$ $Z2 = i\cdot\omega\cdot L_{n2}$ $Z3 = \frac{1}{i\cdot\omega\cdot C_n}$

In this case the capacitance for given equivalent circuit is [16]:

$$C_n = \left((4.386\cdot ln(\varepsilon)+2.33)\cdot\frac{W_2}{W_1} - 5.472\cdot ln(\varepsilon) - 3.17\right)\cdot\sqrt{W_1\cdot W_2}$$

For example, for the frequency *f = 1 GHz*, C_n = *0.046 pF*

The sum inductance:

$$L_C = h\cdot\left(40.5\cdot\left(\frac{W_2}{W_1}-1\right) - 32.57\cdot ln\frac{W_2}{W_1} + 0.2\cdot\left(\frac{W_2}{W_1}-1\right)^2\right)$$

For example, for the frequency *f = 1 GHz*, L_C = *0.219 nH*

Inductances for given equivalent circuit are:

$$L_{n1} = \frac{L_{W1}}{L_{W1}+L_{W2}}\cdot L_C$$ For example, for the frequency *f = 1 GHz*, L_{n1} = *0.067 nH*

$$L_{n2} = \frac{L_{W2}}{L_{W1}+L_{W2}}\cdot L_C$$ For example, for the frequency *f = 1 GHz*, L_{n2} = *0.152 nH*

where L_{W1}, L_{W2} – inductance per unit length of lines 1 and 2.

Let us take as the *ABCD*-parameters of the sample the calculated *ABCD*-parameters of a microstrip transmission line being *0.5 mm* wide with a length of *11 mm* made of copper, $ABCD_2$.

We compute the *ABCD* matrix of the "holder with the sample":

$$\begin{bmatrix} A & B \\ C & D \end{bmatrix}_S = \begin{bmatrix} A & B \\ C & D \end{bmatrix}_1 \cdot \begin{bmatrix} A & B \\ C & D \end{bmatrix}_2 \cdot \begin{bmatrix} A & B \\ C & D \end{bmatrix}_3$$

Let us now find the S-parameters of the "holder with the sample" [16].

$$S_{11} = \frac{A \cdot Z_{02} + B - C \cdot Z_{01} \cdot Z_{02} - D \cdot Z_{01}}{A \cdot Z_{02} + B + C \cdot Z_{01} \cdot Z_{02} + D \cdot Z_{01}}$$

$$S_{12} = \frac{2 \cdot (A \cdot D - B \cdot C) \cdot \sqrt{Z_{01} \cdot Z_{02}}}{A \cdot Z_{02} + B + C \cdot Z_{01} \cdot Z_{02} + D \cdot Z_{01}}$$

$$S_{21} = \frac{2 \cdot \sqrt{Z_{01} \cdot Z_{02}}}{A \cdot Z_{02} + B + C \cdot Z_{01} \cdot Z_{02} + D \cdot Z_{01}}$$

$$S_{22} = \frac{-A \cdot Z_{02} + B - C \cdot Z_{01} \cdot Z_{02} + D \cdot Z_{01}}{A \cdot Z_{02} + B + C \cdot Z_{01} \cdot Z_{02} + D \cdot Z_{01}}$$

where $Z_{01} = Z_{02} = Z_0 = 50\ Ohm$

Since the sample holder has significant dimensions for centimeter wavelengths (Fig. 1), at frequencies above *3 GHz*, the experimental spectrum for S_{21} deviates significantly from the model, as a result, only measurements made in the frequency range up to *3 GHz* can be considered. In addition, at frequencies below *3 GHz*, the magnitude of the modulus of the measured parameter S_{21} is less than the calculated one, which indicates losses in the ferromagnetic sample (Fig. 5). Fig. 6 shows experimental moduli of parameters S_{21} and S_{11} of the holder with sample for selected values of an external magnetic field of *0, 24, 48, 72, 96 and 120 Oe.*

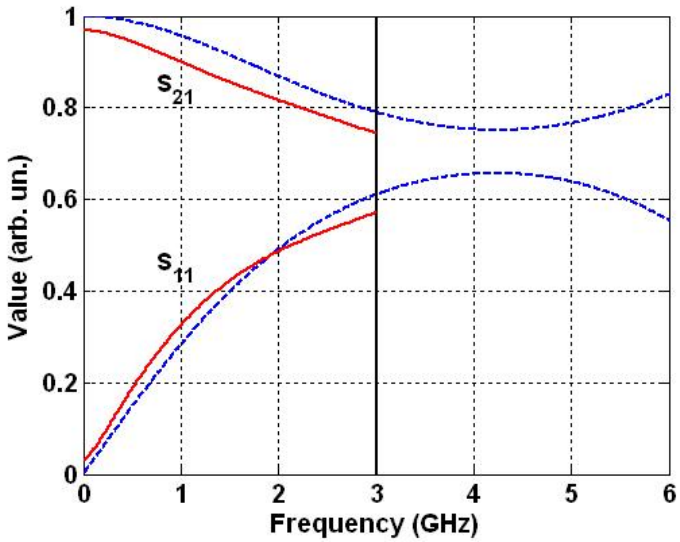


Fig. 5. Calculated (dotted line) and measured with VNA (solid line) moduli of parameters S_{21} and S_{11} of the holder with sample without external magnetic field

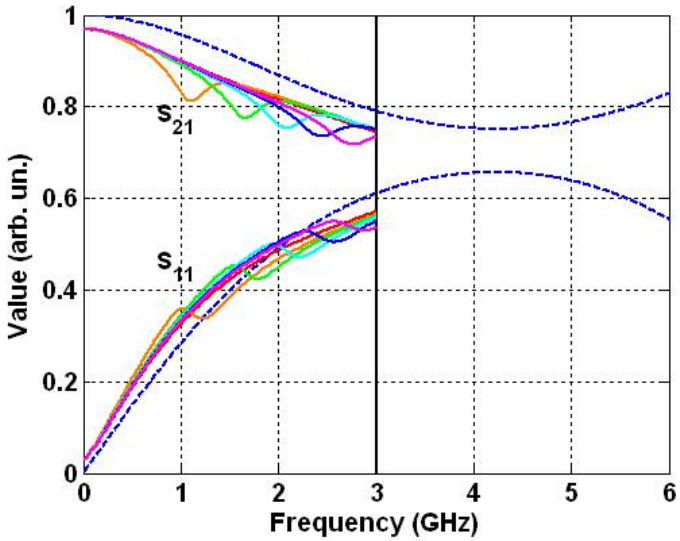


Fig. 6. Experimental (measured with VNA) moduli of parameters S_{21} and S_{11} of the holder with sample with external magnetic field *0, 24, 48, 72, 96* and *120 Oe*. This parameters corresponds to the sample holder and the sample itself

2.3.5. Determination of sample parameters in the frequency range of 0.1 to 6 GHz

Let us calculate matrix of *ABCD*-parameters from the *S*-parameters using well known relations for the stripe of ferromagnetic film [15].

The *ABCD* matrix of the central stripe can be written as follows:

$$\begin{bmatrix} A & B \\ C & D \end{bmatrix}_2 = \begin{bmatrix} A & B \\ C & D \end{bmatrix}_1^{-1} \cdot \begin{bmatrix} A & B \\ C & D \end{bmatrix}_S \cdot \begin{bmatrix} A & B \\ C & D \end{bmatrix}_3^{-1}$$

Considering the sample as a transmission line, we find the requested parameters: the impedance of the sample Z and line propagation constant γ:

$$Z = \sqrt{\frac{B_2}{C_2}} \qquad e^{\gamma} = \sqrt{A_2 \cdot D_2} + \sqrt{B_2 \cdot C_2}$$

Using the relations:

$$Z = \sqrt{\frac{R + i \cdot \omega \cdot L}{G + i \cdot \omega \cdot C}} \qquad \gamma = \sqrt{(R + i \cdot \omega \cdot L) \cdot (G + i \cdot \omega \cdot C)}$$

We can now find the parameters of the line *R, L, G, C*. From the propagation constant γ we find the losses α and the phase coefficient β:

$$\gamma = \alpha + i \cdot \beta; \;\; \alpha = Re(\gamma); \;\; \beta = Im(\gamma);$$

We can now find the series resistance per unit length of the sample series inductance per unit length (L), shunt conductance per unit length (G) and shunt capacitance per unit length (C):

$$R = \alpha \cdot Z \qquad L = \frac{\beta \cdot Z}{\omega} \qquad G = \frac{\alpha}{Z} \qquad C = \frac{\beta}{\omega \cdot Z}$$

Frequency dependences of R, L, G and C parameters are shown in Fig. 7.

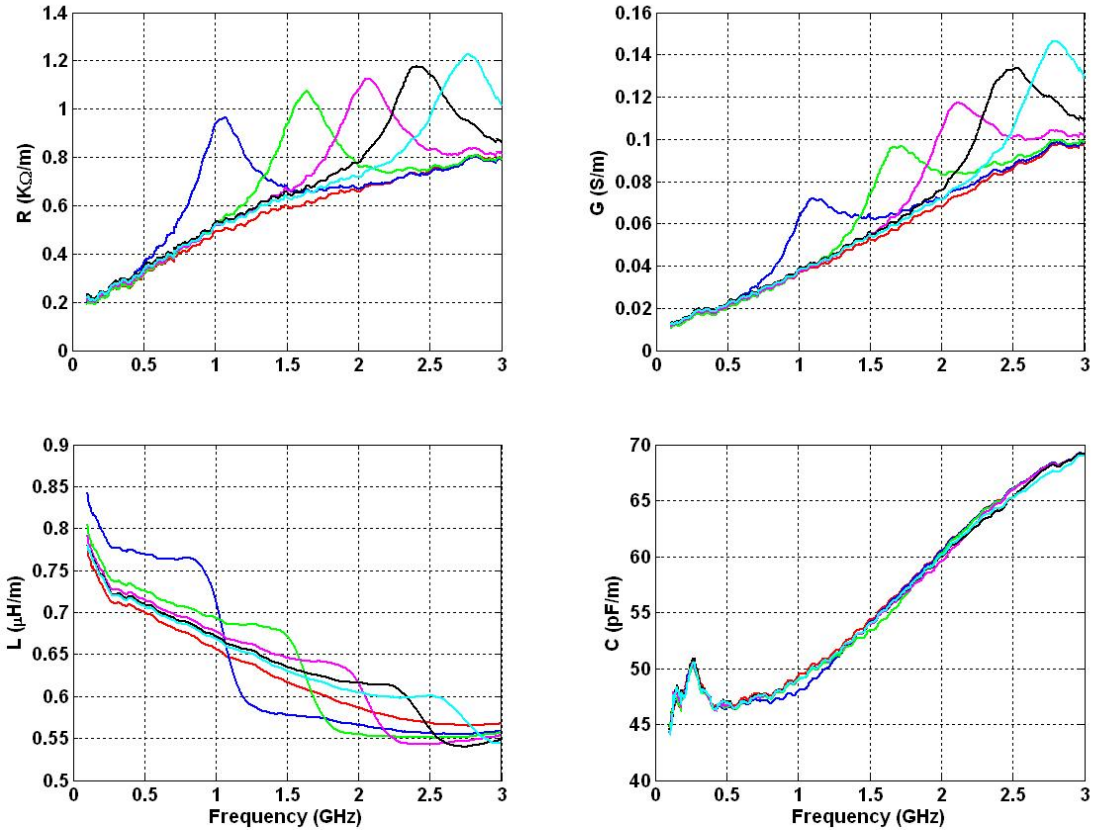


Fig. 7. Frequency dependences of resistance (R) inductance (L), conductivity (G) and capacitance (C) per unit length for ferromagnetic stripe FeNi(70 nm)Cu(3 nm) FeNi(70 nm)/Cu(500 nm)/FeNi(70 nm)Cu(3 nm)FeNi(70 nm) multilayer.

Since the sample itself is a line with a ferromagnetic coating, the most important parameters are the resistance and the inductance when an external constant magnetic field is applied. As the next step one can subtract the background (the value of corresponding parameter for an external field equal to *0*) and obtain the increments of the resistance (ΔR) and the inductance (ΔL) of the studied ferromagnetic stripe (Fig. 8 and Fig. 9 accordingly).

Since a ferromagnet is a medium with losses for electromagnetic waves, the relative magnetic permeability can be represented in a complex form: $\mu = \mu' + \mu''$.

The increments of the resistance ΔR is proportional to μ'' and it characterizes the radiation losses in a ferromagnet. The increments of the inductance ΔL is proportional to μ' and it characterizes the change in the energy of the magnetic field in the sample. It is well known from the classic ferromagnetic resonance theory [18, 19] that at the FMR conditions μ'' reaches the maximum value and μ' changes the sign. Fig. 8 and Fig. 9 convinsingly show that even with such approximate initial calculations and simple sample holders, the curves ΔR and ΔL are close to the classic frequency dependences of μ'' and μ'. A noticeable decrease in the values in the low-frequency branch of μ' with an increase of the external constant magnetic field, can be attributed to a decrease in the magnetic permeability upon saturation of the ferromagnet.

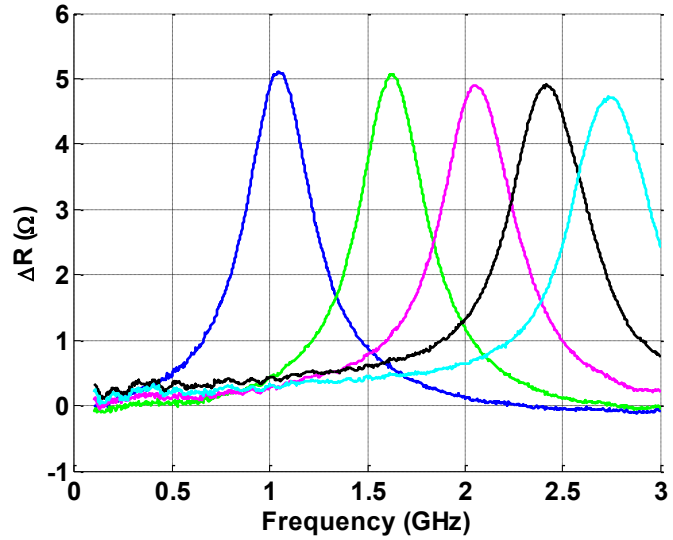


Fig. 8. Frequency dependences of the increments of the resistance for ferromagnetic stripe FeNi(70 nm)Cu(3 nm)FeNi(70 nm)/Cu(500 nm)/FeNi(70 nm)Cu(3 nm)FeNi(70 nm) multilayer

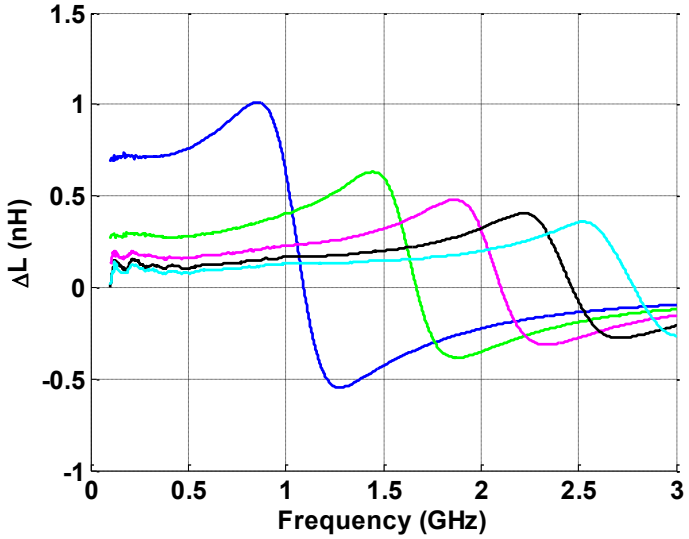


Fig. 9. Frequency dependences of the increments of the inductance for ferromagnetic stripe FeNi(70 nm)Cu(3 nm)FeNi(70 nm)/Cu(500 nm)/FeNi(70 nm)Cu(3 nm)FeNi(70 nm) multilayer

3. CONCLUSIONS

In this work, we have analysed the entire microwave path consisting of the sample holder and the FeNi-based multilayered stripe sample. We had proposed the way for the extracting of the parameters of a transmission line formed by a sample on the substrate. The phenomenon of resonant absorption of electromagnetic waves in the multilayered stripe sample in the external applied magnetic field was carefully investigated. The experimental absorption curves were in a good agreement with the known FMR responses for real and imaginary parts of dynamic magnetic permeability. Designed installation procedure of extracting of the parameters of transmission line can be useful for characterization of magnetic nanostructures designed for sensor applications.

ACKNOWLEDGMENT

This work was supported by the Russian Federation State assignment 3.6121.2017. We thank V.N. Lepalovskij and V.O. Vas'kovskiy for special support.

REFERENCES

1. Beach, R.S., Berkowitz, A.E., Sensitive field- and frequency dependent impedance spectra of amorphous FeCoSiB wire and ribbon, J.Appl.Phys.76 (1994) 6209–6213.
2. Uchiyama, T., Mohri, K., Panina, L.V., and Furuno, K., Magneto-Impedance in Sputtered Amorphous Films for Micro Magnetic Sensor, IEEE Trans. Magn., 1995, vol. 31, no. 6, pp. 3182–3184.
3. Antonov, A.S., Gadetskii, S.N., Granovskii, A.B., et al., Giant Magnetic Impedance in Amorphous and Nanocrystalline Multilayers, *Fiz. Met. Metalloved.*, 1997, vol. 83, no. 6, pp. 61–71.
4. Makhotkin, V.E., Shurukhin, B.P., Lopatin, V.A., et al., Magnetic Field Sensors Based on Amorphous Ribbons, *Sens. Actuat. A*, 1991, vol. 27, pp. 759–762.
5. Nakai, T., Takada, K., Abe, H., et al., Magnetic Field Measurement Using Step-like GMI Sensor Combined with Differential Circuit, *J. Magn. Soc. Jap.*, 2007, vol. 31, pp. 216–220.
6. Kurlyandskaya, G.V., Fernández, E., Svalov, A.V., Burgoa Beitia, A., García-Arribas, A and Larrañaga, A 2016, Flexible thin film magnetoimpedance sensors. Journal of Magnetism and Magnetic Materials, vol. 415, pp. 91–96
7. Correa, M.A., Bohn F., Chesman C., R.B. da Silva, Viegas A.D., Sommer R.L., Tailoring the magnetoimpedance effect of NiFe/Ag multilayer, J.Phys.D:Appl. Phys.43 (2010) 295004–295007.
8. Fernández, E, Svalov, A.V., García-Arribas, A., Feuchtwanger, J, Barandiaran, J.M. and Kurlyandskaya, G.V. High performance magnetoimpedance in FeNi/Ti nanostructured multilayers with opened magnetic flux. Journal of Nanoscience and Nanotechnology, 2012. Vol. 12, pp. 7496–7500
9. Bhagat, S.M., Metals Handbook, ninth ed., vol. 10, American Society of Metals, Metals Park, OH, 1986, p. 267.
10. Srinivasu, V.V., Lofland, S.E., Bhagat, S.M., Ghosh, K., Tyagi, S.D. Temperature and field dependence of microwave losses in manganite powders, J.Appl.Phys. 86 (1999) 1067–1072.
11. Voughan, R.G. Two-port higher mode circular microstrip antennas. IEEE Trans. Antenna Propagation. 1988. 36(3) 309-321.
12. White, J.F. High Frequency Techniques: An Introduction to RF and Microwave Engineering. Hoboken, NJ, USA: IEEE Press, 2004.
13. Svalov, A.V., Gonzalez Asensio, B., Chlenova, A.A., Savin, P.A., Larrañaga, A., Gonzalez, J.M. and Kurlyandskaya, G.V. Study of the effect of the deposition rate and seed layers on structure and magnetic properties of magnetron sputtered FeNi films. Vacuum, 2015. Vol. 119, pp. 245-249
14. Kurlyandskaya, G.V., Kammouni, R. E., Volchkov, S.O., Shcherbinin, S.V., Larrañaga, A. Magnetoimpedance sensitive elements based on CuBe/FeCoNi electroplated wires in single and double wire configurations. IEEE Transactions on Magnetics, 2017. Vol. 53, No. 4.
15. Pozar D.M. Microwave Engineering. Forth ed. John Wiley & Sons, Inc. 2012.
16. Gupta, K.C., Garg, R., Chadha, R. Computer-aided Design of Microwave Circuits. Artech House, Inc. 1981.
17. Gupta, K.C., Garg, R., Bahl, I., Bhartia, P. Microstrip Lines and Slotlines. Second ed. Artech House, Inc. 1996.

18. Kittel, Charles (15 January 1948). On the Theory of Ferromagnetic Resonance Absorption. Physical Review. 73 (2): 155–161
19. Gurevich, A.G., Melkov, G.A. Magnetization Oscillations and Waves. CRC Press, Inc. 1996.